Front. Earth Sci. 2017, 11(1): 63–75
DOI 10.1007/s11707-016-0564-5

RESEARCH ARTICLE

Investigation of the spatiotemporal variation and influencing factors on fine particulate matter and carbon monoxide concentrations near a road intersection

Zhanyong WANG[1], Qing-Chang LU (✉)[1], Hong-Di HE[2], Dongsheng WANG[1], Ya GAO[1], Zhong-Ren PENG (✉)[1,3]

1 Center for ITS and UAV Applications Research, State Key Laboratory of Ocean Engineering, School of Naval Architecture, Ocean & Civil Engineering, Shanghai Jiao Tong University, Shanghai 200240, China
2 Logistics Research Center, Shanghai Maritime University, Shanghai 201306, China
3 Department of Urban and Regional Planning, University of Florida, Gainesville, FL 32611-5706, USA

Abstract The minute-scale variations of fine particulate matter ($PM_{2.5}$) and carbon monoxide (CO) concentrations near a road intersection in Shanghai, China were investigated to identify the influencing factors at three traffic periods. Measurement results demonstrate a synchronous variation of pollutant concentrations at the roadside and setbacks, and the average concentration of $PM_{2.5}$ at the roadside is 7% (44% for CO) higher than that of setbacks within 500 m of the intersection. The pollution level at traffic peak periods is found to be higher than that of off-peak periods, and the morning peak period is found to be the most polluted due to a large amount of diesel vehicles and unfavorable dispersion conditions. Partial least square regressions were constructed for influencing factors and setback pollutant concentrations, and results indicate that meteorological factors are the most significant, followed by setback distance from the intersection and traffic factors. CO is found to be sensitive to distance from the traffic source and vehicle type, and highly dependent on local traffic conditions, whereas $PM_{2.5}$ originates more from other sources and background levels. These findings demonstrate the importance of localized factors in understanding spatiotemporal patterns of air pollution at intersections, and support decision makers in roadside pollution management and control.

Keywords traffic-related pollutants, fine-scale variation, distance gradient, meteorology, road intersection

Received May 2, 2015; accepted October 26, 2015

E-mail: qclu@sjtu.edu.cn (Qing-Chang LU), zrpeng@sjtu.edu.cn (Zhong-Ren Peng)

1 Introduction

Roadside has been regarded as a seriously polluted area posing adverse health threats from exposures to traffic-related air pollutants (HEI, 2010), but is a place where people spend a significant amount of their daily outdoor time (Kaur and Nieuwenhuijsen, 2009). In particular, road intersections and their surroundings are more contaminated due to a high emission rate resulting from the geometrical characteristics of intersected roads and big variations in traffic flow (e.g., free, interrupted, congested) and vehicular state (e.g., idle, acceleration, deceleration, cruise) (He et al., 2009; Soulhac et al., 2009; Mazzeo and Venegas, 2012). It is also reported that the impact of major roads on air quality is significant within a range of up to 500 m distance (HEI, 2010). Such a range could cover a wide area of dense population around an intersection, and air pollution is thus of great concern to these people.

There are plenty of studies that have been conducted to estimate traffic-related air pollution. Most of them focused on pollutant emissions and distributions around roadways, by different transportation modes, or at transit stops, but few studies addressed air pollution around an intersection as it is more complex for the dispersion of air pollutants with many uncertainties (Soulhac et al., 2009; Kellnerova and Janour, 2011; Tiwary et al., 2011). A limited number of studies at road intersections mainly concentrate on three aspects: field observations, wind tunnel experiments, and numerical simulations (Tiwary et al., 2011). Due to the difficulty in data acquisition, field studies are even fewer, which is actually important for urban planners, designers, and government officials to better understand the pollution pattern around an intersection. Recently, the project group

of "dispersion of air pollution and penetration into the local environment" (DAPPLE) launched tens of field measurements in the vicinity of a street intersection in central London, focusing on the effects of wind on pollutant dispersion (Shallcross et al., 2009; Tomlin et al., 2009; Martin et al., 2010a, b), and Mazzeo and Venegas (2012) related the ambient wind with NO_x concentrations and wind speed/direction measured in a street canyon close to an intersection. These studies well present the associations of air pollutants with roof-top or ground wind at intersections, but do not address traffic effects on air pollution patterns. With these considerations, only a few studies have been conducted among the literature reviewed. Pandian et al. (2009) reported the effects of traffic and road characteristics on vehicle emissions, and He and Lu (2012) explained the variations of particles of different sizes at a roadside affected by traffic and weather factors. The relationship between traffic signal timing and fine particle concentrations on sidewalks was also discussed by Slavin and Figliozzi (2013). Recently, Wang et al. (2015a, b) proposed a set of hybrid methods to estimate the fine-scale $PM_{2.5}$ and CO variations near road intersections.

Current studies have preliminarily described the distribution pattern of air pollutant concentrations at intersections and unveiled the underlying determinants, while there are still many things unknown. For instance, previous roadside measurements include pedestrian exposures to air pollutants when walking near the road, however, situations in neighborhoods where many residences are exposed to the pollution are rarely known. Apart from the wind, other meteorological factors such as air temperature, dew-point temperature, relative humidity, and air pressure are often highly correlated with each other and jointly affect the local pollution level (Jian et al., 2012). Consequently, there are still some challenges to reach agreements on how these correlated factors affect street-scale pollutant variation in a statistical sense. Moreover, as the traffic-related emission intensity and local meteorology are variable, air pollutants around an intersection can significantly vary at minute scale (Zito et al., 2008; Galatioto and Zito, 2009; Soulhac et al., 2009; Tiwary et al., 2011; He and Lu, 2012). Studies further found that short-term exposures (e.g., minutes) to high pollutant levels are even more serious compared to long-term general exposures (e.g., annual, monthly, daily) (Brook et al., 2002; Grivas and Chaloulakou, 2006). Hence, the fine-scale estimation of air pollution becomes important for decision makers who can take measures at an intersection or its surrounding built environment to reduce pollution risk. To date, little attention has been paid to the short-time variation of air pollutants, and the major factors that contribute to variations have not been well known (He et al., 2009; Soulhac et al., 2009; Martin et al., 2010a, b; Tiwary et al., 2011; Jian et al., 2012; Farrell et al., 2014; Zhang et al., 2014).

To fill the void, we carried out field measurements near a road intersection in Shanghai, China, to provide additional insights into the minute-scale concentration variation of two air pollutants characterized by different nature — i.e., fine particulate matter ($PM_{2.5}$) and carbon monoxide (CO) — from the roadside to nearby setbacks. We attempt to identify the main factors that affect the concentration variability over three traffic periods, and hope to shed light on the development of effective strategies for pollution control and air quality management at roadsides.

2 Field experiment and data collection

2.1 Field experiment

A suburban site (31°1'N, 121°26'E) in Shanghai, China, was selected for data collection, which involves a busy signalized intersection crossed by Dongchuan Rd. (4 lanes) and Cangyuan Rd. (2 lanes) (see Fig. 1(a)). The air pollutants were monitored simultaneously at both roadside (the white dot at the bottom right of Fig. 1(a)) and setbacks (the white dots with numbers (No.1–3) in Fig. 1(a)). The roadside site lay on the sidewalk along the campus of Shanghai Jiao Tong University (SJTU), and setbacks sat on the SJTU campus 110 m, 330 m, and 500 m from the intersection. The SJTU campus was selected for setback layout because it is an open space from roadside to setbacks without high buildings blocking the dispersion of pollutants, which is ideal to evaluate the immediate effects of local traffic emissions on neighborhoods. Three setbacks characterize different spatial locations from the intersection, which helps to understand the distance gradient effects of air pollution distributions.

2.2 Data collection

The field data collection lasted for four sunny days in spring 2013, and based on a traffic survey as well as the statistical results of this measurement shown in Fig. 1(b), daily measurement was split into morning (07:00–09:00), midday (11:00–14:00), and afternoon (16:00–18:00) periods. Morning and afternoon periods are regarded as peak traffic periods while midday is identified as the off-peak period.

The actual pollution level varies remarkably at fine-time scales around intersections (Zito et al., 2008), and thus $PM_{2.5}$ ($\mu g/m^3$) and CO (ppm (parts per million)) were measured at minute level in this study. Two sets of portable monitors were used to detect both pollutants at roadside and setbacks. The monitors were set up 1.7 m above the ground which is close to the breathing zone of adult pedestrians. Minute-by-minute $PM_{2.5}$ concentrations were collected using a TSI Sidepak AM510 instrument based on light-scattering technique. Five-second instantaneous CO concentrations were recorded by Langan T15n electrochemical sensors, and then one 1-min sample was obtained

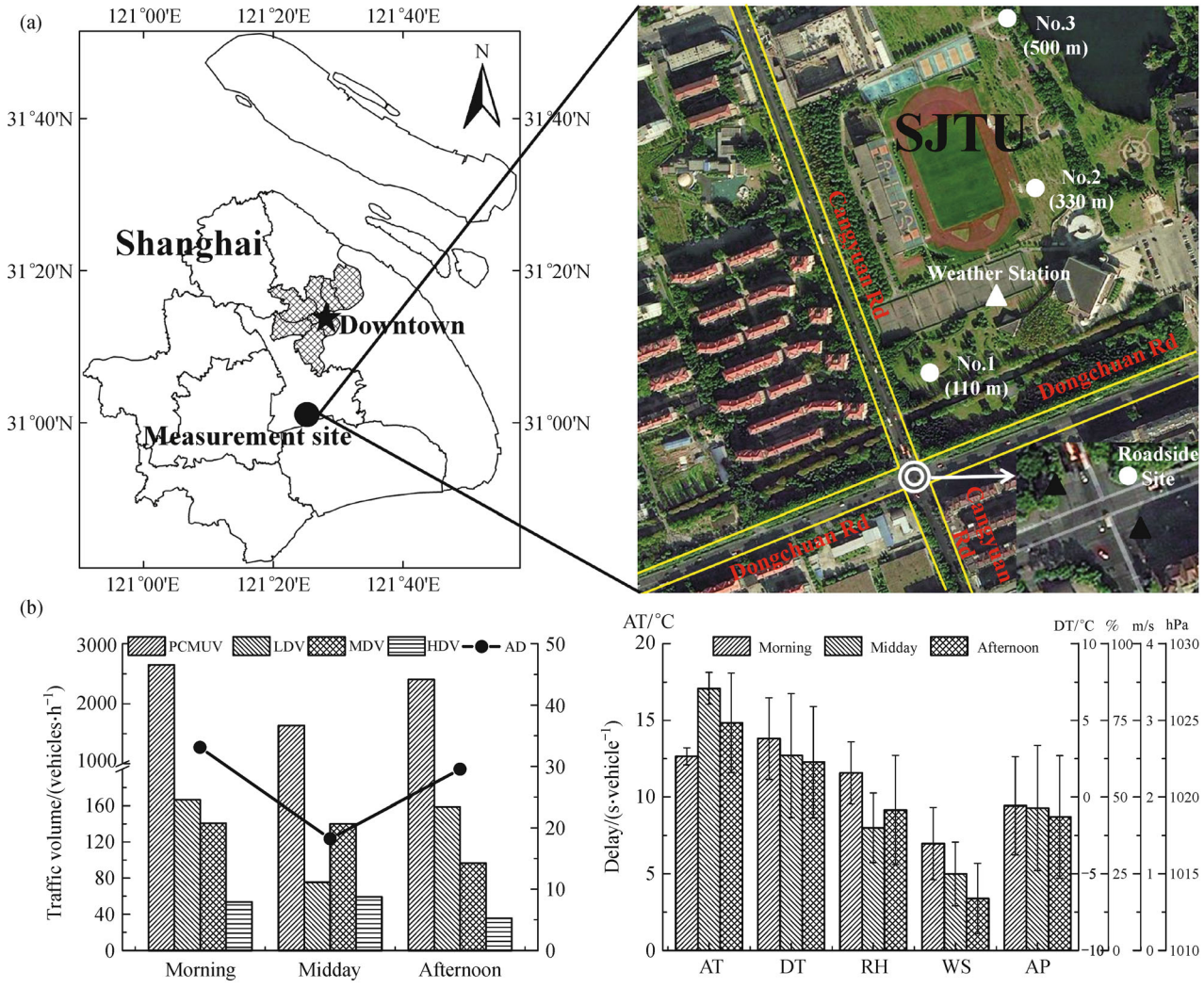

Fig. 1 Schematic of field measurement: (a) experiment layout near an intersection site; (b) hourly average conditions of traffic and meteorology at the intersection. Note: In Fig.1(a), the white circle demonstrates the intersection connected by four road segments from directions of east, south, west, and north. In Fig. 1(b), PCMUV, LDV, MDV, and HDV denote the traffic volume of four categories of vehicles, i.e., passenger cars and medium-utility vehicles (e.g., taxi, jeep), light-duty vehicles (e.g., coach, bus), medium-duty vehicles (e.g., truck), and heavy-duty vehicles (e.g., trailer), respectively; AD denotes average delay of the whole intersection; AT (°C), DT (°C), RH (%), WS (m/s), and AP (hPa) represent air temperature, dew-point temperature, relative humidity, wind speed, and air pressure, respectively.

by averaging 20 continuous observations. Prior to this field experiment, all the portable devices used here were first calibrated before leaving the factory and then further verified on the basis of collocated standard methods at outdoor locations in Shanghai. Finally, roadside monitoring lasted for four experimental days, while two days' data was collected at No. 1 (110 m) setback, and data collection continued for one day at No. 2 (330 m) and No. 3 (500 m) setbacks. It is noted that we only had two sets of portable instruments for roadside and setback measurements, and thus background measurements were missed. Fortunately, the four experimental days were sunny with the similar pollution background and meteorology reported by the official online results. From the measurements, we also found a similar pollution level among the four days, where the daily $PM_{2.5}$ and CO are about 60 μg/m^3 and 0.8 ppm, respectively, based on average values of continuous roadside monitoring results. For these reasons, we assume little impact from the daily background variations on our study results.

At a street-scale traffic environment, air pollution depends heavily on traffic, meteorology, and spatial locations (Buonanno et al., 2011). Two cameras (two black triangles in the lower right of Fig. 1(a)) were used to record traffic conditions, and traffic variables were manually counted for each of the four road segments as

shown in Fig.1(a). A 5-min sampling interval was chosen for comparison among the four road segments, as well as considering that it is a significantly stable fine-time scale to reduce sampling randomness. According to the vehicle structure and fuel types, traffic volumes (vehicles/5 min) were subdivided into four categories of vehicles: PCMUV, LDV, MDV, and HDV as defined in Fig. 1. A longer queue length can cause a longer stay of vehicles on roads, and then more emissions (Galatioto and Zito, 2009). Hence, queue length on four road segments (vehicles/5 min) was recorded separately during the red traffic light. Queue length is defined as the length of stopping cars starting from the stop line, the equal of the number of stopping PCMUV on one lane of a segment where the other three types of vehicles mentioned above were converted into the reference type of PCMUV based on Transportation Research Board's Highway Capacity Manual. Besides queue length, we counted the total number of stopping cars on all lanes of each segment. The average delay (seconds/vehicle) on each segment was then calculated as the total delay on the segment (i.e., a product of the total number of stopping cars and phase length of the red light) divided by the total number of vehicles on the segment. The average delay of the whole intersection was then defined as the sum of the total delay on the four segments divided by the total number of stopping vehicles. As shown in Fig. 1(b), traffic flows were characterized by two peaks of morning and afternoon periods with total traffic volumes of 57% and 41%, respectively, which are larger than that of midday (about 1900 vehicles/hour). In regard to vehicle composition, the gasoline-based PCMUV dominated the traffic, while the diesel-fueled vehicles were less than 15%, and HDV accounted for less than 3% of the total traffic. The average delay (AD) characterizing overall traffic condition was higher in peaks, particularly in the morning, than that of the midday period.

Local meteorology of air temperature (AT), relative humidity (RH), wind speed (WS), wind direction (WD), dew-point temperature (DT), and air pressure (AP) was recorded at 1-min scale by a Davis Vantage Weather Station mounted 2.5 m above the ground on the SJTU campus (the white triangle in Fig. 1(a)) and about 200 m away from the intersection. As illustrated in Fig. 1(b), WS ranged from 0 to 2.4 m/s over the sampling period and decreased gradually from morning to afternoon. WS was 1.5 times higher in the morning than in the afternoon. WD, even with low WS (0 m/s for an exception), was found to be variable with time throughout the observation. As a result, the sampling positions covered both upwind and leeward of the intersection. Besides, AT and RH exhibited opposite patterns, whereas both AP and DT had slight decreases from morning to afternoon. In general, such significant time-based variations of meteorological factors are likely to increase the complexity of pollutant dispersion at the street scale.

3 Methodology

3.1 Data

In the field experiment, more than 24 hours of observations were conducted with approximately two hours for each individual period of day. Due to the accidental failure and out-of-sync equipment, parts of the data are invalid or lost. First, we dropped the invalid data which are out of mean value ± 3 standard deviation, and 1140 groups of 1-min samples of pollutants and meteorology as well as 166 groups of 5-min traffic records were retained. Second, pollutants and meteorology data were unified to the timestamp of the traffic series with a 5-min interval, which is a rather stable interval to reduce sampling randomness based on previous studies (Zhu et al., 2002) where five continuous 1-min samples were regularized into a 5-min average. After data processing, a total of 136 groups of 5-min samples for all variables are available for analysis.

Since the wind direction was originally measured as angles (°), for computational purpose as well as to make measurement comparable between setbacks, a measurement called relative wind direction (RWD) was defined in this study. First, a coordinate system was built with the intersection as origin and clockwise azimuth ranging from 0° to 359°, and 0° denotes north along the meridian line. Second, a line was drawn linking the intersection with setbacks, and its clockwise angle from north was calculated. Third, the angle (0° to 180°) of that linking line was computed with the measured wind direction (i.e., WD). RWD is equal to –1 when the angle is 0° with 0 corresponding to 90° and 1 to 180°. When RWD increases from –1 to 1, the angle increases from 0° to 180°. Note that the measured wind direction indicates the wind blowing to the coordinate origin.

3.2 Statistical analysis

Before statistical analysis, *X*- and *Y*-variables with a range of more than one magnitude of 10 were logarithmically transformed to make their distributions fairly symmetrical (Wold et al., 2001).

3.2.1 Wilcoxon rank-sum test

The Wilcoxon rank-sum test is a powerful non-parametric test usually used when data are distributed abnormally or when it is unsure whether data follow a normal distribution (Hollander and Wolfe, 1999). Here, it is used to analyze the differences of air pollutant observations between different time periods of day. As noted by He and Lu (2012), two sets of samples need to be combined into one set and sorted in an increasing order, and then the sum of ranks is calculated with the following formula:

$$W = \sum_{i=1}^{n} R_i - \frac{n(n+1)}{4}, \quad (1)$$

where n is sample size, and R_i denotes rank for i^{th} observation. If two populations have the same distribution, the sum of the two sample ranks should be close to the same value. In this study, a Z-statistic was used to compute the approximate two-sided p-value for testing the null hypothesis that the two distributions are at the same confidence level. In this study, Wilcoxon rank-sum tests were implemented in the software SAS.

3.2.2 Partial least square regression (PLSR)

PLSR is an improvement of the linear regression and the principal component regression. PLSR can take into account the information of X-variables and Y-variables simultaneously and overcome adverse effects of collinearity in the modeling. In this study, PLSR models were run separately at three time periods to identify relationships of the potential explanatory variables (i.e., X-variables including all 20 variables of traffic, meteorology, and distance measured here) with $PM_{2.5}$ or CO measurements (i.e., Y-variables including mass concentrations of setback $PM_{2.5}$ or CO). The principle of PLSR is detailed by Wold et al. (2001).

Cross validation (CV) is used to identify the number of significant PLS components. For component a, CV (renamed as Q^2) is calculated with the following equation:

$$Q_a^2 = 1 - \frac{PRESS_a}{SS_{a-1}}, \quad (2)$$

where $PRESS_a$ denotes the prediction error sum of squares of component a, and SS_{a-1}denotes the fitted residual sum of squares of component a–1. Generally, if Q_a^2 is lower than 0.0975, the component a becomes insignificant, and then the model refuses to introduce this component. Together with the coefficient of determination (R^2), the cumulative CV (i.e., Q_{cum}^2) of all extracted components can estimate the goodness-of-fit and stabilization of PLSR. Moreover, PLSR is better built when Q_{cum}^2 is larger than 0.5 and R^2 is closer to 1.

In order to identify the importance of variables explaining Y (Wold et al., 2001), the variable importance for projection (VIP) is developed with the following equation:

$$VIP_k = \sqrt{\sum_{a=1}^{A}(w_{ak}^2(SSY_{a-1} - SSY_a))}\frac{K}{SSY_0 - SSY_A}, \quad (3)$$

where k is the serial number of X-variables, K is the total number of X-variables, A is the number of significant components of PLSR, w_{ak}^2 is the squared PLSR weight of k^{th} variable of component a, SSY_{a-1}, SSY_a is the explained residual sum of squares of Y of component a–1 and a, respectively, and $SSY_0 - SSY_A$ is the total residual sum of squares of Y explained by the PLSR model. The bigger the VIP value, the more important the X-variable is. Furthermore, a VIP value larger than 1 indicates the most relevant factor explaining Y, and a VIP value lower than 0.5 indicates an unimportant X-variable. The interval between 1 and 0.5 is a grey zone where the importance level depends on the size of the data set. In this paper, PLSR models were constructed using the software SIMCA-P version 11.5.

4 Results and discussion

4.1 Spatiotemporal variations of $PM_{2.5}$ and CO concentrations near the intersection

Based on mean values of four days' observations, Figure 2(a) illustrates one-minute sequences of $PM_{2.5}$ and CO concentrations during three time periods at roadside and setbacks without distinguishing varied setback locations. From Fig. 2(a), three key points can be summarized. First, concentrations of both pollutants are higher at the roadside than at setbacks over three time periods. The average drops are approximately 7% for $PM_{2.5}$ and 44% for CO from roadside to setbacks. Relative to a big fall-off for CO, a moderate $PM_{2.5}$ reduction likely has to do with secondary production or high background contribution. The different nature of such factors as transport pathway and diffusion intensity for the two pollutants may also contribute to a different gradient (HEI, 2010). Comparing the gradients of pollutants concentrations observed in this study with previous studies near major roads, both similarities and dissimilarity exist. For example, Zhu et al. (2002) reported a slight drop (about 10%) for mass concentrations of total PM, but a sharp decrease (about 90%) for CO concentrations at 300 m from a freeway. Beckerman et al. (2008) depicted a varying decay degree of $PM_{2.5}$ (20%–60%) at 500 m from two expressways. McAdam et al. (2011) found that hourly $PM_{2.5}$ was 39% higher at 10 m from curb side than that of 30 m from curb side, but there was no significant difference in CO levels with increasing distance from the road. Our research is generally consistent with near-road studies that $PM_{2.5}$ levels in neighborhoods are lower than at the roadside. However, the remarkable difference of the decreasing $PM_{2.5}$ amplitudes and CO gradients is probably because of the different study design, field traffic volumes, and meteorological conditions (Beckerman et al., 2008). Second, a synchronous variation is identified at roadside and setbacks, but it is more obvious for $PM_{2.5}$ than CO, especially in afternoon peak hours. This implies that CO is sensitive to local traffic since it mainly comes from real-time vehicular emissions at street scale (Hagler et al., 2010), while $PM_{2.5}$ is likely dependent more on background levels and other sources (HEI, 2010; Zhang et al., 2014). Third, the pollution level is higher in traffic peaks

than midday (also see Table 1), which demonstrates that local pollution variability is more related to traffic conditions. Moreover, the pollutant concentration is higher in the morning than the afternoon, agreeing with findings of field measurements of particles with different sizes in China (Jian et al., 2012; Zhang et al., 2014).

As Table 1 shows, statistical analyses were used to assess the differences between two sets of observations. The Shapiro-Wilk test result as well as skew and kurtosis with values far from zero indicate that the measured $PM_{2.5}$ and CO are non-normal distributions, especially at setbacks. As learned from the results of the Wilcoxon rank-sum test (see Table 2), $PM_{2.5}$ distributions are similar in midday and afternoon, but different in the morning at 5% significance level. This can be explained by two evidences below. Figure 1(b) shows that the average relative humidity is 58%, 40%, and 46% in the morning, midday, and afternoon, respectively. Hence, the coagulation process of $PM_{2.5}$ is enhanced in the morning, which poses an inevitable influence on $PM_{2.5}$ background levels (He and Lu, 2012). In addition, traffic volumes were larger in the morning than during midday and afternoon periods, and there were more diesel trucks and trailers in the morning, which would emit more particulates compared with other vehicle types (Wang et al., 2011).

To identify the local spatial gradient of pollution variation, we normalized the $PM_{2.5}$ and CO concentrations measured from three setbacks to the roadside based on upwind and downwind conditions of the intersection (Fig. 2(b)). Figure 2(b) shows that mean concentrations of both pollutants decline more at 110 m and 500 m than 330 m for both wind directions. As seen from Fig. 1(a), different local surroundings at the three setbacks are likely responsible for the results. At 110 m, a sharp drop of pollutant concentration, especially for CO, is likely because of some sort of obstruction from trees between the roadside and this setback. The 500 m setback is the farthest from the intersection and beside a lake with lake breezes, which might explain that a maximum attenuation ratio of pollutants appears at this setback. An unobvious decline of pollutant concentration is found at the 330 m setback. This setback is located in an open field near a playground that has a more homogeneous and stable atmosphere than the other two locations, and thus is less affected by direct traffic emission. The correlation analysis in Table 3 indicates that there are strongly positive correlations

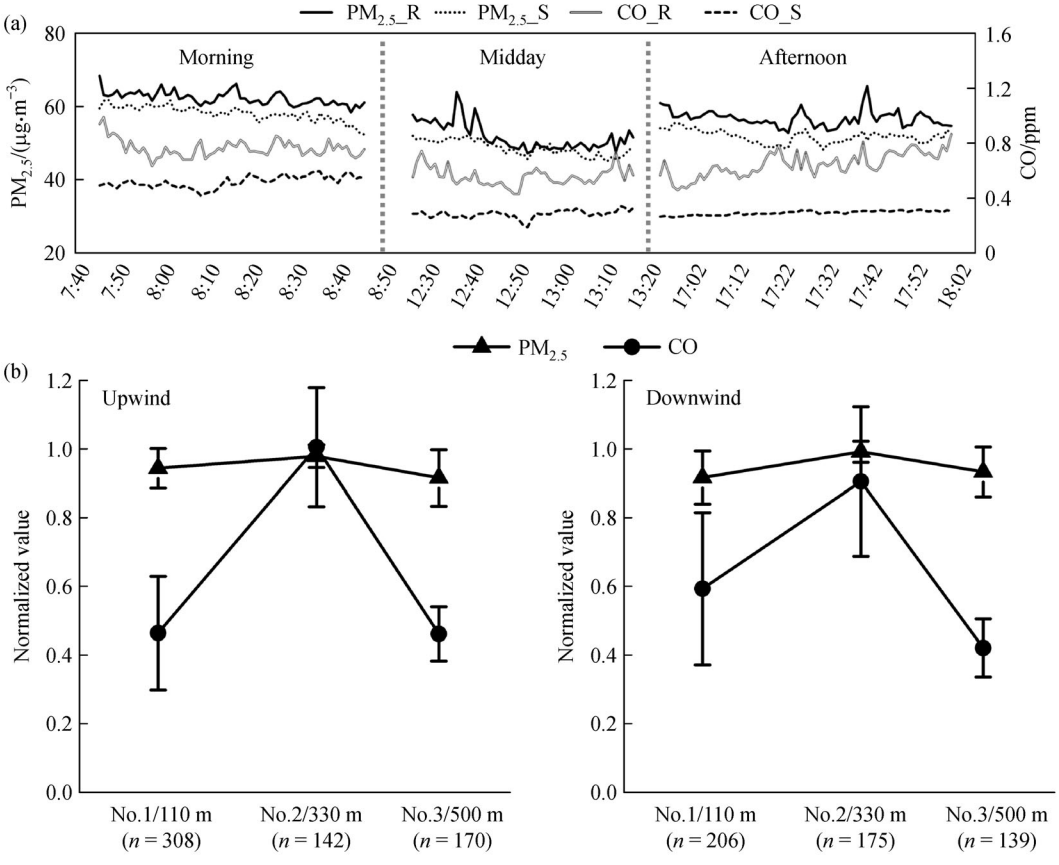

Fig. 2 Comparison of $PM_{2.5}$ and CO concentrations from the roadside to setbacks: (a) 1-min series, (b) normalized setback $PM_{2.5}$ and CO levels (±1 standard deviation) to roadside measurements. Note: $PM_{2.5}$_R (or CO_R) and $PM_{2.5}$_S (or CO_S) represent roadside and setback $PM_{2.5}$ (or CO) concentration, respectively. In Fig. 2(b), *n* indicates the number of samples at three setbacks.

Table 1 Basic statistics for minute samples of $PM_{2.5}$ and CO concentrations with time periods and locations

	Time periods	Mean	SD	Range	Skew	Kurtosis	Shapiro-Wilk test	
							W	$P < W$
$PM_{2.5}$_R	Morning	62.29	20.17	63.23	−0.52	−1.07	0.88	0.000
	Midday	51.81	13.06	39.45	−0.72	−0.83	0.85	0.000
	Afternoon	56.75	19.06	55.91	0.18	−1.66	0.87	0.000
$PM_{2.5}$_S	Morning	58.16	18.59	59.97	−0.39	−1.04	0.90	0.001
	Midday	48.67	13.85	41.98	−0.80	−0.79	0.83	0.000
	Afternoon	51.78	19.72	54.11	0.31	−1.64	0.84	0.000
CO_R	Morning	0.76	0.28	1.55	−0.31	0.25	0.95	0.044
	Midday	0.56	0.16	0.87	0.83	2.17	0.95	0.045
	Afternoon	0.65	0.13	0.48	0.14	−0.87	0.96	0.138
CO_S	Morning	0.52	0.20	0.88	−0.12	−0.67	0.95	0.049
	Midday	0.29	0.14	0.45	0.72	−1.00	0.85	0.000
	Afternoon	0.30	0.15	0.43	0.60	−1.20	0.84	0.000

Note: $PM_{2.5}$_R (μg/m^3) and $PM_{2.5}$_S (μg/m^3) indicate $PM_{2.5}$ concentrations at the intersection and setbacks, respectively; CO_R (ppm) and CO_S (ppm) indicate CO concentrations at the intersection and setbacks, respectively. Mean and SD denote average value and standard deviation, respectively; Range is a measure of variation; Skew and Kurtosis are used to identify an asymmetrical distribution or not. Shapiro-Wilk test (i.e., normal distribution test) is presented with the W statistic and p-value (i.e., $P < W$) for each group of pollutant variable. The statistical calculation is implemented in the software of Statistical Analysis System (SAS). The number of samples is 387, 371, and 382 in morning, midday, and afternoon periods, respectively.

Table 2 Wilcoxon rank-sum test for minute samples of setback $PM_{2.5}$ and CO concentrations with time periods

	Time periods	Sum of scores	Expected	Wilcoxon statistic	$P < Z$
$PM_{2.5}$_S	Morning	2066	1566	2066	0.000
	Midday	1675	2175		
	Morning	1989	1566	1989	0.000
	Afternoon	1752	2175		
	Midday	2391	2525	2391	0.357
	Afternoon	2659	2525		
CO_S	Morning	2208	1566	2208	0.000
	Midday	1533	2175		
	Morning	2249	1566	2249	0.000
	Afternoon	1492	2175		
	Midday	2889	2525	2889	0.012
	Afternoon	2161	2525		

Note: $PM_{2.5}$_S (μg/m^3) and CO_S (ppm) indicate setback $PM_{2.5}$ and CO concentrations, respectively. Wilcoxon rank-sum test for setback $PM_{2.5}$ and CO concentrations between different time periods is given with some key indicators, where the p-value (i.e., $P < Z$) indicates significance degree. The statistical calculation is implemented in the software of Statistical Analysis System (SAS). The number of samples is 387, 371, and 382 in morning, midday, and afternoon periods, respectively.

between concentrations of both pollutants with setback distance in the afternoon period, which is opposite to the other two time periods of day. This implies that the spatial gradient of pollutant level may also be related to time-based impacts of regional background or other sources. With the factors described above, the pollution distribution does not seem to follow an obvious distance-decay gradient within 500 m, and a similar result was reported for $PM_{2.5}$ within 50 m of an arterial road in Shanghai (Zhang et al., 2014). As seen from Fig. 2(b), the closer the distance from the intersection becomes, the bigger the standard deviation (SD) of the normalized setback pollutant level is. This suggests that the contribution of roadway traffic emission on the nearby pollutant level generally decreases with the increase of distance from the intersection. Such phenomenon is more prominent for CO than $PM_{2.5}$, further suggesting a higher sensitivity of CO to local traffic emission. The direct contribution of traffic emission to $PM_{2.5}$ concentration near the roadway is small through the above analysis, which coincides with previous study results on roadside particles (Zhu et al., 2002, 2006). Moreover, Figure 2(b) denotes a slightly bigger SD for the normalized setback pollutant concentration downwind than upwind of the intersection. As summarized by Zhu

Table 3 Pearson correlations between influencing factors and setback $PM_{2.5}$ and CO concentrations

	$PM_{2.5}$			CO		
	Morning	Midday	Afternoon	Morning	Midday	Afternoon
DS	**−0.75**	**−0.38**	**0.90**	−0.15	−0.05	**0.77**
AT	−0.20	**−0.32**	**0.68**	**0.61**	**0.54**	**0.67**
RH	**−0.62**	**0.34**	**−0.3**	**−0.89**	−0.16	**−0.50**
WS	−0.23	**0.55**	**0.58**	0.02	**−0.55**	**0.52**
RWD	**−0.64**	**−0.55**	**0.91**	−0.21	**0.35**	**0.91**
DT	**−0.69**	0.20	0.08	**−0.85**	**−0.46**	−0.16
AP	**0.88**	−0.08	**−0.49**	**0.79**	**0.64**	**−0.29**
PCMUV	**0.41**	−0.04	**0.29**	0.05	0.13	**0.32**
LDV	0.18	0.27	0.16	−0.18	−0.14	0.20
MDV	0.20	−0.10	0.23	0.04	−0.13	0.26
HDV	−0.17	0.09	0.17	0.04	−0.13	0.12
ADEW	0.01	**−0.46**	**0.59**	−0.04	**0.67**	**0.69**
ADWE	0.27	−0.12	0.00	−0.01	0.04	0.04
ADSN	0.26	**−0.38**	0.11	0.17	**0.64**	0.22
ADNS	0.23	**−0.40**	0.21	0.01	0.19	0.24
AD	0.32	**−0.54**	**0.42**	−0.00	**0.58**	**0.53**
QLEW	0.09	**−0.33**	**0.50**	0.02	**0.64**	**0.60**
QLWE	**0.53**	−0.19	0.10	0.01	0.00	0.15
QLSN	0.30	−0.22	0.13	0.08	0.21	0.21
QLNS	0.15	−0.04	−0.02	−0.14	0.27	0.04

Note: The bold denotes the significance at 5% level (2-tailed). DS indicates setback distance from the intersection; RWD indicates relative wind direction as defined earlier; ADEW, ADWE, ADSN, and ADNS indicate average delay of the link from east to west, west to east, south to north, and north to south, respectively; QLEW, QLWE, QLSN, and QLNS indicate queue length of the link from east to west, west to east, south to north, and north to south, respectively. Other variable abbreviations are defined in Fig.1.

et al. (2006), the altered direction of the wind thus is vital to be taken into account to accurately estimate near-roadway pollutant exposures.

In summary, the $PM_{2.5}$ and CO concentration patterns near the intersection depend on the time of day or variables associated with time of day. The joint effect of many factors causes different levels of pollutants at the varied setbacks of the intersection.

4.2 Identification of influencing factors on $PM_{2.5}$ and CO concentrations at setbacks

PLSR modeling of setback $PM_{2.5}$ and CO concentrations was carried out at a 5-min scale so as to better understand the complex interaction of pollutant concentration variation with variables of interest. The results of observed and predicted $PM_{2.5}$ and CO standardized values (i.e., logarithmically transformed values) at three time periods are presented in Fig. 3, in which all the models constructed are significant at the 5% level. R^2 values for $PM_{2.5}$ and CO models reach 0.9 or so at most time periods, indicating that the models explain about 90% of $PM_{2.5}$ or CO variation. For $PM_{2.5}$, the model established was the most accurate in the morning, followed by the afternoon, and the least accurate in midday with an R^2 of 0.69. This could be explained by the idea that a less varied background $PM_{2.5}$ level and relative stable meteorological factors in the morning may be more accurately represented by local modeling, while in the midday and afternoon, the $PM_{2.5}$ modeling has an increasing randomness due to frequently varied meteorological conditions and emissions from various regional and nearby sources with the increase of human activities. A weak model built for the midday data also likely resulted from a rapid decline of local traffic flow but a rising impact of meteorology and other uncertain factors. In contrast, all CO models are well built with less fluctuation among the time periods. The midday model is slightly better than models of other time periods. It can be interpreted that the rapid decline of local traffic emission leads to a small range of CO measurements and little contribution from other sources because of a big attenuation rate of CO with distance. Nevertheless, all Q^2 values are greater than 0.5, demonstrating the reliability of the PLSR model for assessing the impacts of measured factors on both pollutants.

Based on the well-constructed PLSR models, variable importance for the projection (VIP) was calculated to test the importance of each factor explaining $PM_{2.5}$ and CO

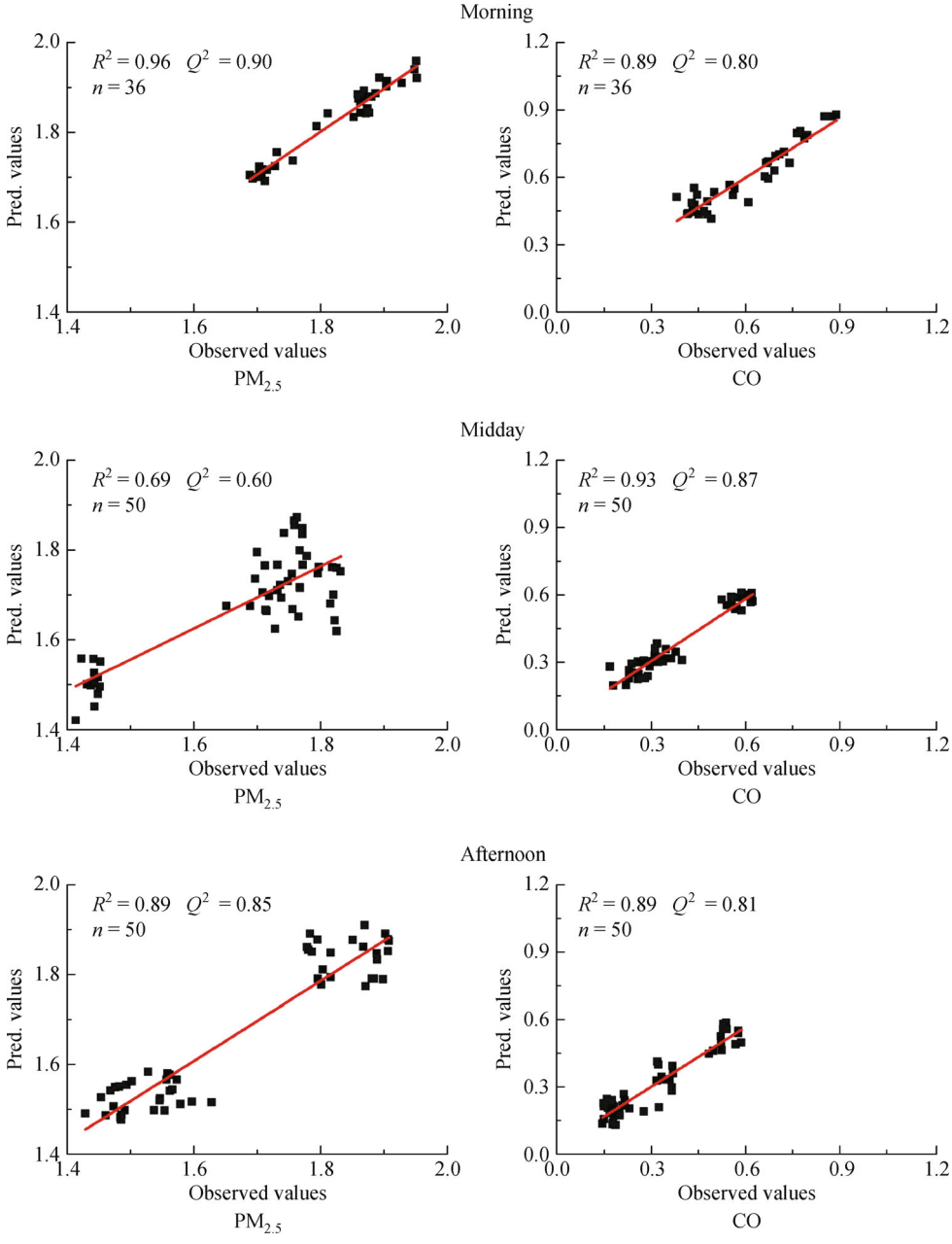

Fig. 3 Standardized $PM_{2.5}$ and CO observations vs. PLSR predictions at three time periods (*n* denotes the number of samples).

variations (see Fig. 4). On the whole, both $PM_{2.5}$ and CO are strongly dependent on meteorology factors and setback distance from the intersection since most of them have VIP values bigger than 1. Several traffic factors show observably important effects on the pollutant concentrations, but the majority get VIP values around 0.5, showing less contributions. However, those features mentioned above vary with traffic periods and two pollutants. Together with Pearson correlation coefficients in Table 3, the impacts of factors on the pollutants are discussed below.

DS always stands in the first group (VIP bigger than 1) with prominent influence on $PM_{2.5}$ in all periods, and its interaction with CO gradually increases from morning to afternoon. The two pollutants have different dispersion features, and thus different distance-gradient patterns during the day. From Table 3, correlations of DS with both pollutants are negative in the morning and midday, indicating distance decay effects as also reported by HEI (2010). But it becomes positive in the afternoon, which shows the effects of other sources on field measurements (Zhang et al., 2014).

Among the meteorological factors, air temperature (AT) has a strong positive correlation with pollutant levels for most of the time periods. The field campaign was carried out in sunny days with strong sunlight, and therefore it is

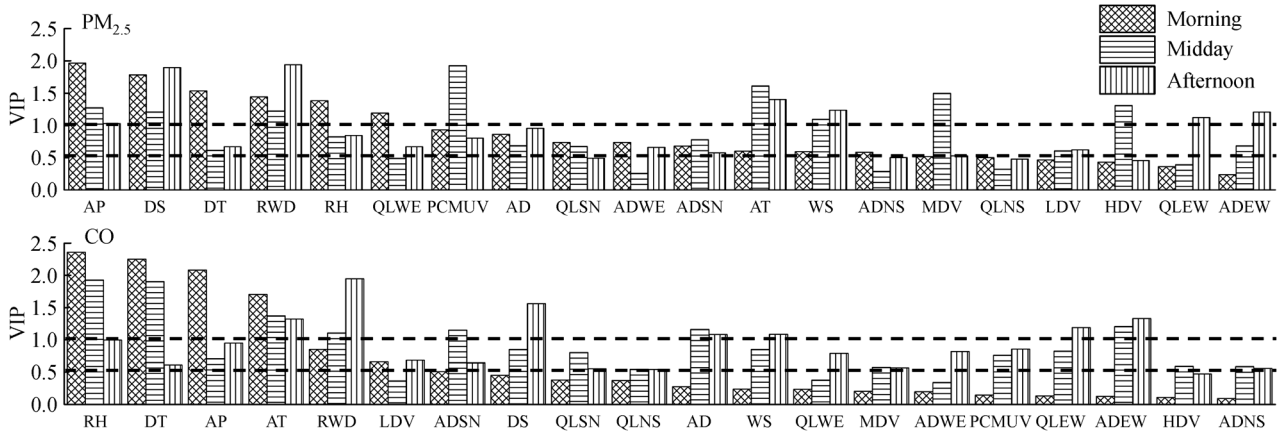

Fig. 4 Variable importance for the projection (VIP) of $PM_{2.5}$ and CO models at three time periods (in order of VIP from largest to smallest values based on morning results). Note: All the variable abbreviations are consistent with the definitions in Table 3.

likely that an increase in secondary $PM_{2.5}$ is transformed by co-pollutants (e.g., O_3, NO_x, and SO_2) as the AT rises. This is also reported by Jian et al. (2012), that the atmospheric process was responsible for the positive relation of the AT with roadside submicron particles, which might also act on the increase of CO concentrations.

Contrary to the AT, relative humidity (RH) is negatively related to $PM_{2.5}$ or CO in most periods. Recently, researches also reported that traffic-related air pollutants (e.g., $PM_{2.5}$, ultra-fine particles, and other particles with smaller size) were inversely proportional to RH (Yli-Tuomi et al., 2005; Yao et al., 2007; Jamriska et al., 2008; Farrell et al., 2014). These results differ from typical regional environment studies, and a possible reason is related to the complex traffic environment. For example, $PM_{2.5}$ originates from not only exhaust emissions but also road dust, brakes, and tires in addition to other mechanical sources (Yli-Tuomi et al., 2005; HEI, 2010). It is not difficult to understand that RH could increase the surface wetness of particles and thus suppress the road dust generation. Meanwhile, these multiple-source-based particles can also grow by coagulation and/or condensation of gases with the increase of RH, and then easily be deposited near the road rather than diffusing to neighborhoods. High RH also likely changes the local photophysical and photochemical reaction between CO and other air pollutants, especially in our experimental days with high solar radiation and warm weather, and thus causes a loss of CO. For example, Jia and Xu (2014) reported that in the gas phase of secondary organic aerosol formation, the decrease of CO with the increase of RH can mainly be explained by the uptake of glyoxal into the wall or the aerosol phase.

As can be seen from Fig. 4, the effects of wind speed (WS) and relative wind direction (RWD) are significant and gradually increase from morning to afternoon. As shown in Table 3, the correlation of WS with the pollutants has different values and signs over the day, suggesting that WS plays an unstable role of diluting or increasing pollutant concentrations. RWD is significantly correlated to $PM_{2.5}$ or CO (at 5% level) in almost all time periods, but the sign varies between positive and negative. In the morning traffic peak period, both WS and RWD are negatively correlated with setback pollutants most of the time. This result indicates that the high wind speed is effective for diluting and reducing high concentrations of the pollutants, which is similar to previous near-road pollution exposure studies (Hagler et al., 2010; Buonanno et al., 2011; Jian et al., 2012; Farrell et al., 2014). In addition, there are emission sources from the campus direction (northeast of the intersection in Fig. 1(a)) increasing the pollution levels of all setbacks, and the Xin-Feng-Jin highway lying about 1000 m northeast of the intersection may be an important source. Conversely, WS and RWD show positive associations with the pollutants at 5% significance level in the afternoon peak, indicating that the area downwind of the intersection is increasingly polluted as wind speed increases. As a result, a positive significant impact of traffic emissions on neighborhoods is implied at the selected intersection. As Fig. 1(b) shows, wind speed gradually weakens from morning to afternoon. A higher wind speed plays a role in diluting high background levels of the pollutants in the morning, whereas in the afternoon, all the setback locations are dominated by the breeze which brings more pollution with the increase of local traffic volumes. In midday, the reversed sign of WS (or RWD) correlated with $PM_{2.5}$ and CO depends on different formations of the two pollutants. The correlation of $PM_{2.5}$ is positive with WS, but negative with RWD. This further indicates the influence of the highway emission source from the campus direction, and higher wind speed benefits a long-distance transport of particles to the field measurement site. In contrast, CO is mainly affected by local traffic emission, and lower wind

speed is in favor of its dispersion to the neighborhood, which is due to its high decay ratio with distance, unlike $PM_{2.5}$ with the long-distance transport feature.

Dew temperature (DT) is an indicator linking the AT with RH and is found to be negatively correlated to the pollutants, especially CO, similar to the relation of both pollutants with RH. It can be concluded that DT represents more information of RH although it also reflects the characteristics of the AT. One interesting finding from this study is that the correlation of air pressure (AP) with both pollutants varied over time periods. As Jian et al. (2012) said, AP strongly affects the levels of pollutants in the way of formation, growth, movement, or dispersion, and the underlying mechanism is complex. Additionally, AP is mixed with the AT, RH, and DT, which have a complex causal relationship.

Traffic factors also explained the pollutant concentration variation over time. In the morning, traffic factors fall far behind meteorological factors and DS, and catch up slightly in the other two periods (Fig. 1 and Table 3). As dominant vehicle types (seen from Fig. 1(b)), passenger cars and medium-utility vehicles (PCMUV) are significantly correlated with the pollutants (particularly $PM_{2.5}$) in the morning and afternoon traffic peaks. Traffic volumes of other vehicle types have less contribution to the pollutant concentration, but they highlight a relative importance in midday compared with other periods. We also find from the figures and tables that the pollution variation at setbacks is closely related to traffic conditions on some segments as well as time periods. But most traffic variables have low VIP, even less than 0.5, suggesting that they are not important and can be ignored. For instance, the average delay and queue length from north to south along Cangyuan Rd., i.e., ADNS and QLNS, are identified as unimportant. It is interpreted that during the entire day there is almost no congestion in this direction with an indistinct data fluctuation, and thus unobvious correlations with the pollutants are observed in Table 3. The weak role of LDV (i.e., various buses) is also observed in PLSR models, which demonstrates the advantage of PLSR compared to conventional regressions, i.e., effectively overcoming colinearity between LDV and PCMUV.

In summary, the joint effect of spatial location, meteorological factors, local traffic variables, and other uncertain sources plays a crucial role in street-scale variations of $PM_{2.5}$ and CO concentrations, which is in accordance with previous studies on roadside air pollutants (McAdam et al., 2011; Jian et al., 2012). Moreover, different variables are found having different effects on both $PM_{2.5}$ and CO concentrations, and the impact of the same variable varies dramatically among time periods. The regular or irregular impacts of factors on air pollutants have preliminarily pointed to the subtle associations of these factors with pollutants in intersection microenvironments, although further work is needed to quantify such results in much more detail. In addition, the importance of localized factors in understanding spatiotemporal patterns of air pollutant levels around road intersections has been highlighted in this study, which can help decision makers to take effective measures to relieve the daily health risk in these microenvironments in the future by delineating proper setback requirements to certain land use types and implementing certain design elements.

5 Conclusions

Based on field measurements of $PM_{2.5}$ and CO concentrations near a road intersection in Shanghai, China, this study characterized minute-scale variations of the two pollutants and provided insights into the effects of dynamic factors at three time periods of day. Drawn from measurement data, the decrease of average concentration is about 7% for $PM_{2.5}$ and 44% for CO from roadside to setbacks within 500 m from the intersection. Local traffic emissions are found to have significant impacts on the setback pollution level, but differences are observed between the two pollutants due to their different properties, e.g., the transport pathway and diffusion mechanism. CO variation is sensitive to traffic factors and distance from the traffic source, while the secondary product and high background concentration produced by other sources may be critical for $PM_{2.5}$ concentration. Pollutant concentrations are higher in traffic peaks than off-peak periods and greater in the morning than the afternoon. This is substantially related to local traffic and micro-climate in real time. Concentrations of both pollutants have obvious distance decay within the first 110 m, beyond which the pattern is not that obvious and needs further investigations. To unveil interactions of variables of interest with pollutants at different time periods, partial least square regressions for setback $PM_{2.5}$ and CO were established at a 5-min scale. Results indicate that pollutant levels strongly depend on micro-meteorology which determines the dispersion of vehicular pollutants, followed by distance from the intersection, and most traffic factors rank behind. The strong joint effect of most measured variables and other factors, such as uncertain sources and background, plays a decisive role in variations of setback $PM_{2.5}$ or CO levels.

Although we have highlighted the importance of localized factors in understanding the air pollution pattern near an intersection, this study still has its limitations. More samples with full features such as periodic (e.g., seasonal, weekly, daily) are expected to refine the current study. The field campaign needs to be improved by increasing spatial sampling locations so that a detailed spatial gradient of pollutant levels can be observed. To verify different performances of various pollutants at fine-time scale, future research should consider more pollutants such as ultrafine particles, black carbon, carbon dioxide,

and ozone. Furthermore, it should be examined whether the results found in this paper can be extended to other sites in future studies.

Acknowledgements This work was sponsored by the Peking University-Lincoln Institute (DS20120901), the Shanghai Environmental Protection Bureau (No. 2014-8) and the State Key Laboratory of Ocean Engineering (GKZD 010059) at Shanghai Jiao Tong University, and the National Natural Science Foundation of China (11302125). We would like to thank members from the Shanghai Environmental Monitoring Center for their assistance in the instrumental calibration, and a special appreciation is expressed to colleagues from the Center for ITS and UAV Applications Research at Shanghai Jiao Tong University for their hard work in data collection and processing. We also acknowledge Wina Meyer and Alissa Meyer from the International Friendship of the University of Florida and Trina Burgess from the Department of Geography at the University of Lethbridge for their proofreading on our manuscript. Finally, we appreciate the anonymous reviewers' insightful comments on our work.

References

Beckerman B, Jerrett M, Brook J R, Verma D K, Arain M A, Finkelstein M M (2008). Correlation of nitrogen dioxide with other traffic pollutants near a major expressway. Atmos Environ, 42(2): 275–290

Brook R D, Brook J R, Urch B, Vincent R, Rajagopalan S, Silverman F (2002). Inhalation of fine particulate air pollution and ozone causes acute arterial vasoconstriction in healthy adults. Circulation, 105(13): 1534–1536

Buonanno G, Fuoco F C, Stabile L (2011). Influential parameters on particle exposure of pedestrians in urban microenvironments. Atmos Environ, 45(7): 1434–1443

Farrell W, Weichenthal S, Goldberg M, Hatzopoulou M (2014). A statistical model explaining air pollution exposures of cyclists in urban environments. Proceedings of the 93rd Annual Meeting of the Transportation Research Board, Washington, DC, January

Galatioto F, Zito P (2009). Traffic parameters estimation to predict road side pollutant concentrations using neural networks. Environ Model Assess, 14(3): 365–374

Grivas G, Chaloulakou A (2006). Artificial neural network models for prediction of PM10 hourly concentrations, in the Greater Area of Athens, Greece. Atmos Environ, 40(7): 1216–1229

Hagler G S W, Thoma E D, Baldauf R W (2010). High-resolution mobile monitoring of carbon monoxide and ultrafine particle concentrations in a near-road environment. J Air Waste Manag Assoc, 60(3): 328–336

He H D, Lu W Z (2012). Urban aerosol particulates on Hong Kong roadsides: size distribution and concentration levels with time. Stochastic Environ Res Risk Assess, 26(2): 177–187

He H D, Lu W Z, Xue Y (2009). Prediction of PM10 concentrations at urban traffic intersections using semi-empirical box modelling with instantaneous velocity and acceleration. Atmos Environ, 43(40): 6336–6342

HEI (2010). Traffic-related air pollution: a critical review of the literature on emissions, exposure, and health Effects. HEI Special Report 17, Health Effects Institute, Boston, MA

Hollander M, Wolfe D A (1999). Nonparametric Statistical Methods. Hoboken, NJ: John Wiley & Sons, Inc

Jamriska M, Morawska L, Mergersen K (2008). The effect of temperature and humidity on size segregated traffic exhaust particle emissions. Atmos Environ, 42(10): 2369–2382

Jia L, Xu Y (2014). Effects of relative humidity on ozone and secondary organic aerosol formation from the photooxidation of benzene and ethylbenzene. Aerosol Sci Technol, 48(1): 1–12

Jian L, Zhao Y, Zhu Y P, Zhang M B, Bertolatti D (2012). An application of ARIMA model to predict submicron particle concentrations from meteorological factors at a busy roadside in Hangzhou, China. Sci Total Environ, 426: 336–345

Kaur S, Nieuwenhuijsen M J (2009). Determinants of personal exposure to $PM_{2.5}$, ultrafine particle counts, and CO in a transport microenvironment. Environ Sci Technol, 43(13): 4737–4743

Kellnerova R, Janour Z (2011). Flow instabilities within an urban intersection. International Journal of Environment and Pollution, 47 (1/2/3/4): 268–277

Martin D, Nickless G, Price C S, Britter R E, Neophytou M K, Cheng H, Robins A G, Dobre A, Belcher S E, Barlow J F, Tomlin A S, Smalley R J, Tate J E, Colvile R N, Arnold S J, Shallcross D E (2010b). Urban tracer dispersion experiment in London (DAPPLE) 2003: field study and comparison with empirical prediction. Atmos Sci Lett, 11(4): 241–248

Martin D, Price C S, White I R, Nickless G, Petersson K F, Britter R E, Robins A G, Belcher S E, Barlow J F, Neophytou M, Arnold S J, Tomlin A S, Smalley R J, Shallcross D E (2010a). Urban tracer dispersion experiments during the second DAPPLE field campaign in London 2004. Atmos Environ, 44(25): 3043–3052

Mazzeo N A, Venegas L E (2012). Hourly NOX concentrations and wind direction in the vicinity of a street intersection. International Journal of Environment and Pollution, 48(1/2/3/4): 96–104

McAdam K, Steer P, Perrotta K (2011). Using continuous sampling to examine the distribution of traffic related air pollution in proximity to a major road. Atmos Environ, 45(12): 2080–2086

Pandian S, Gokhale S, Ghoshal A K (2009). Evaluating effects of traffic and vehicle characteristics on vehicular emissions near traffic intersections. Transp Res Part D Transp Environ, 14(3): 180–196

Shallcross D E, Martin D, Price C S, Nickless G, White I R, Petersson F, Britter R E, Neophytou M K, Tate J E, Tomlin A S, Belcher S E, Barlow J F, Robins A (2009). Short-range urban dispersion experiments using fixed and moving sources. Atmos Sci Lett, 10 (2): 59–65

Slavin C, Figliozzi M A (2013). Impact of traffic signal timing on sidewalk-level particulate matter concentrations. Transportation Research Record, 2340: 29–37

Soulhac L, Garbero V, Salizzoni P, Mejean P, Perkins R J (2009). Flow and dispersion in street intersections. Atmos Environ, 43(18): 2981–2996

Tiwary A, Robins A, Namdeo A, Bell M (2011). Air flow and concentration fields at urban road intersections for improved understanding of personal exposure. Environ Int, 37(5): 1005–1018

Tomlin A S, Smalley R J, Tate J E, Barlow J F, Belcher S E, Arnold S J, Dobre A, Robins A (2009). A field study of factors influencing the concentrations of a traffic-related pollutant in the vicinity of a complex urban junction. Atmos Environ, 43(32): 5027–5037

Wang X, Westerdahl D, Wu Y, Pan X, Zhang K M (2011). On-road emission factor distributions of individual diesel vehicles in and

around Beijing, China. Atmos Environ, 45(2): 503–513

Wang Z, He H D, Lu F, Lu Q C, Peng Z R (2015b). Hybrid model for prediction of carbon monoxide and fine particulate matter concentrations near a road intersection. Transportation Research Record. Journal of the Transportation Research Board, 2503: 29–38

Wang Z, Lu F, He H D, Lu Q C, Wang D, Peng Z R (2015a). Fine-scale estimation of carbon monoxide and fine particulate matter concentrations in proximity to a road intersection by using wavelet neural network with genetic algorithm. Atmos Environ, 104: 264–272

Wold S, Sjostrom M, Eriksson L (2001). PLS-regression: a basic tool of chemometrics. Chemom Intell Lab Syst, 58(2): 109–130

Yao X H, Lau N T, Fang M, Chan C K (2007). Correlations of ambient temperature and relative humidity with submicron particle number concentration size distributions in on-road vehicle plumes. Aerosol Sci Technol, 41(7): 692–700

Yli-Tuomi T, Aarnio P, Pirjola L, Mäkelä T, Hillamo R, Jantunen M (2005). Emissions of fine particles, NO_x, and CO from on-road vehicles in Finland. Atmos Environ, 39(35): 6696–6706

Zhang D Z, Yu Y, Peng Z R (2014). Near-road $PM_{2.5}$ concentration estimation using artificial neural network approach. Proceedings of the 93rd Annual Meeting of the Transportation Research Board, Washington, DC, January

Zhu Y, Hinds W C, Kim S, Sioutas C (2002). Concentration and size distribution of ultrafine particles near a major highway. J Air Waste Manag Assoc, 52(9): 1032–1042

Zhu Y, Kuhn T, Mayo P, Hinds W C (2006). Comparison of daytime and nighttime concentration profiles and size distributions of ultrafine particles near a major highway. Environ Sci Technol, 40(8): 2531–2536

Zito P, Chen H B, Bell M C (2008). Predicting real-time roadside CO and NO_2 concentrations using neural networks. IEEE Trans Intell Transp Syst, 9(3): 514–522